Michigan Technological University

Michigan Technological University
Digital Commons @ Michigan Tech

Department of Physics Publications

Department of Physics

2-1-2000

Fluctuation properties of precipitation. Part VI: Observations of hyperfine clustering and drop size distribution structures in three-dimensional rain

A. R. Jameson
RJH Scientific, Inc.

Alexander Kostinski
Michigan Technological University

Follow this and additional works at: https://digitalcommons.mtu.edu/physics-fp

Part of the Physics Commons

Follow this and additional works at: https://digitalcommons.mtu.edu/physics-fp

Part of the Physics Commons

Fluctuation Properties of Precipitation. Part VI: Observations of Hyperfine Clustering and Drop Size Distribution Structures in Three-Dimensional Rain

A. R. Jameson

RJH Scientific, Inc., Alexandria, Virginia

A. B. Kostinski

Department of Physics, Michigan Technological University, Houghton, Michigan

ABSTRACT

In past work it is argued that rain consists of patches of coherent, physical drop size distributions passing in an unpredictable fashion for an unknown duration over a sensor. This leads to the detection both of correlations among drops and of clustering. While the analyses thus far support this characterization, in this final paper in this series, techniques are developed demonstrating that clustering of drops of a specific size in rain is occurring even on scales as small as a few centimeters. Moreover, using video disdrometer data processed to achieve high temporal resolution, it is shown that drops of different sizes are also cross correlated over times from 0.01 to several seconds.

It is then shown that physical patches of drop size distributions (often exponential in form) exist and can be measured even over time periods as small as 2–3 s. Such distributions may be the result of enhanced drop interactions due to clustering or perhaps simply stochastic "accidents" brought about by some "clustering" mechanism. Since most drop spectra are measured over considerably longer intervals, however, observed distributions are likely probability mixtures of many short duration spectra. Such mixed distributions exhibit enhanced variance and curvatures reminiscent of gamma spectra often described in the literature. Thus, as measurement intervals increase, the form of the observed drop distributions apparently changes from an exponential-like distribution, to a mixture of distributions, finally returning once again to an exponential when the averaging is over very long intervals and a wide variety of conditions.

It is also shown that for these data, much of the variability in rainfall rate arises due to concentration fluctuations rather than to changes in the average drop size. For completeness, it is also shown that the dimensionality of drop counts and rainfall rate are consistent with Euclidean scaling over distances from centimeters to kilometers.

Finally, a specific example of drop clustering in wide sense statistically stationary rain is also given. These observations *cannot* be explained in terms of a nonhomogeneous Poisson process. Consequently, it appears most appropriate to characterize clustering and the structure of rain in terms of correlations and probability ruling discussed here and in previous papers in this series. This approach can be used to simulate rain numerically in order to explore not only the statistical properties of the rain itself, but also to achieve a better understanding of the effect of raindrop clustering and rainfall variability on a variety of topics, such as signal statistics and interpretations of remote sensing measurements.

1. An overview

The curtains of drops sweeping across the pavement as well as the pulsations on the car windshield when driving in rain are common manifestations of the natural "clustering" of raindrops. In previous parts of this series of papers, it is shown that such clustering is an expression of the correlation among the number of drops in one unit volume with those in neighboring unit volumes separated by distance *l*.

Specifically, if we represent the random number of drops of a single size in a unit volume by, say, *n,* then for a statistically homogeneous random field, the joint probability $P(1, 2)$ of finding two particles in small volumes dV_1 and dV_2 is given by (e.g., see Green 1969, 62–63)

$$P(1, 2) = \overline{n}^2 dV_1 \, dV_2 \, [1 + \eta(l)], \qquad (1)$$

where $\eta(l)$ is the so-called pair correlation function (in the theory of liquids) or the two-point correlation function (in astronomy). Note, however, that statistical homogeneity does *not* imply nor require physical homogeneity. "Patchy," physically inhomogeneous rain can be fully consistent with statistical homogeneity. Moreover, it is often assumed in many fields of science that

Corresponding author address: Dr. A. R. Jameson, 5625 N. 32nd St., Arlington, VA 22207-1560.
E-mail: jameson@rjhsci.com

over some interval, usually much greater than some characteristic correlation length, a physical process can be well described by statistical homogeneity (i.e., the mean and the variance are unaffected by shifts in the choice of origin); that is, no "trend" appears, whether it be light years in the case of astronomy or the dimensions of molecules in liquids. One of the objectives for this current work is to push the resolution in rain measurements to even finer limits than in past work in order to extend the entire range considered in this series of papers from a few centimeters to kilometers. It is hoped that this will enhance the likelihood that statistical homogeneity applies to some scale in this range and, therefore, that these results are not some kind of statistical artifact. As we shall see, the findings here not only support, but also amplify previous conclusions.

In practice $\eta(l)$ is estimated operationally from a series of measurements in space by

$$\eta(l) \equiv \frac{\left[\overline{n(l)n(0)} - \overline{n}^2\right]}{\overline{n}^2} = \frac{\overline{n(l)n(0)}}{\overline{n}^2} - 1. \quad (2)$$

This also applies to a time (t) series of observations in which $l = tV$, where V is a known or constant velocity. For rain that is distributed in space such that $n(l)$ are all independent for all l (as would be the case for the Poisson distribution), then, obviously, $\eta \to 0$. However, when $\eta \neq 0$, then we may say that the drops are "correlated" [(1)] and clustered [(2)] in that $\langle n(l)n(0) \rangle$ is either greater or less than $(\overline{n})^2$.

This discussion is not new and has been presented in the previous papers in this series. In Part I (Kostinski and Jameson 1997), several arguments, including (2), indicate that the statistics of drop counts at one size are consistent with the arrival of random patches of random duration. However, it is noted that the "coherency" times at different drop sizes vary. Consequently, in Part II (Jameson and Kostinski 1998), it is shown that η can be modified to become

$$\Omega(l) \equiv \frac{\left[\overline{n_2(l)n_1(0)} - \overline{n}_1\overline{n}_2\right]}{\overline{n}_1\overline{n}_2} = \frac{\overline{n_2(l)n_1(0)}}{\overline{n}_1\overline{n}_2} - 1, \quad (3)$$

where the subscripts refer to drops of two different sizes. As with η, whenever $\Omega \neq 0$, the number of drops at the different sizes are statistically correlated leading to the definition of "drop size distribution" patches, that is, regions in which the drop size spectrum remains coherent. From such correlation we infer that these spectra are "physical" distributions, presumably resulting from the interaction among drops of different sizes. This contrasts with most measured drop size distributions, which are averages over intervals much longer than the coherency lengths of each contributing physical distribution.

The results in Parts I and II, however, are based on 1-min sampling of Joss–Waldvogel (1967) disdrometer observations over several hours corresponding to a minimum spatial sampling of a few hundred to several hundreds of meters. Furthermore, the observations in Part II indicate that the coherency times for the physical drop size distributions are often less than the 1-min sampling available using the Joss–Waldvogel disdrometer. In order to achieve finer resolution, video disdrometer measurements over several minutes are analyzed at 1-s resolution in Part IV (Jameson et al. 1999).

The instrument used in that study is the University of Iowa, Iowa Institute of Hydraulic Research video disdrometer.[1] Briefly, two light sources generate orthogonal light sheets that are projected through narrow slits onto two line scan cameras, that is, horizontal, linear arrays of light sensitive detectors sampled on the order of 30 μs to yield a continuous data stream having no "dead" times. The optics are designed so that, seen through the camera lens, the slits appear evenly and brightly lit. Particles falling through the beams of light appear as dark silhouettes against this background. The light sources and cameras form the sensor unit that is then exposed to the precipitation. Thus, the operation is similar to a flatbed scanner except that the hydrometeors move rather than the line scan camera and light sheet. The effective sample area observed by both cameras is approximately 10 cm × 10 cm or twice that of a Joss–Waldvogel disdrometer. The time series of particle images observed by both cameras are then processed to yield the location (to within 0.2 mm horizontally), size, and other parameters describing the particles. This information is normally integrated from 15 s to hours to yield other quantities such as rainfall rate. However, for our purposes, we instead return to the original stored data and retrieve the recorded time of arrival to the nearest millisecond, as well as the size of each drop to form a time series. In Part IV, these drops are "binned" to yield the number of drops per second in categories 0.25 mm wide in 0.25-mm steps from 0.625 mm up to whatever the largest size happens to be, and to produce statistics of 1-s counts without the masking effects of "ringing" and dead times encountered when using the Joss–Waldvogel disdrometer (Sheppard and Joe 1994).

In Jameson et al. (1999) it is shown that drops of one size are correlated not only down to 1-s times (corresponding to a few to several meters spatially), but also that the coherence times of the physical drop size distributions last often only several tens of seconds. Moreover, since the coherence times of the drop size distributions are determined by the smallest correlation time of the contributing drops, Part IV suggests that some drop size distributions may only be observed over intervals of seconds. Hence, sampling even over 10 s is sometimes likely too coarse to resolve clearly all the physical drop size distribution patches.

This poses two interesting questions: namely, is there

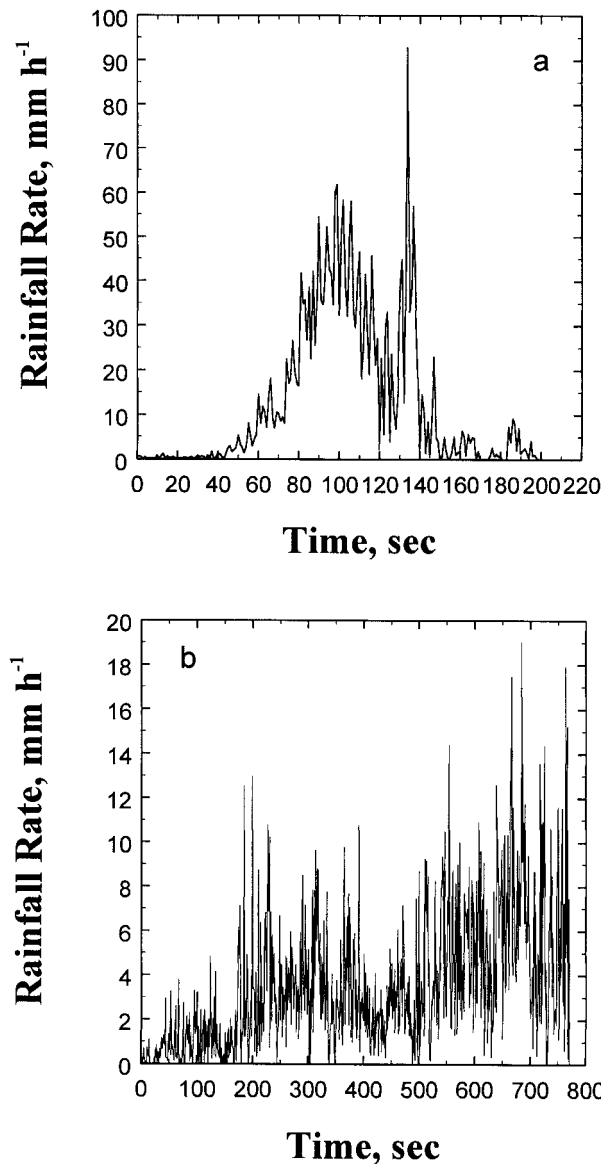[1] Visit http://ias.tu-graz.ac.at/distro.html for further information.

FIG. 1. The 1-s rain rates measured using the University of Iowa video disdrometer during (a) a brief convective shower and (b) a more extended less convective rain.
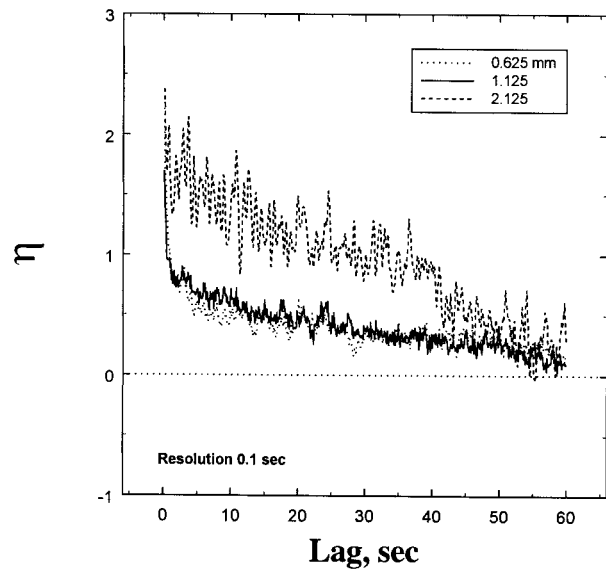

FIG. 2. The pair correlation at three sizes of drops for a temporal counting sample of 0.1 s. The dotted line at zero corresponds to values for Poisson statistics.

some resolution at which clustering is no longer apparent, and what is the finest temporal (spatial) scale over which individual drop size distributions can be associated with real, physical patches, assuming they can be at all? In addressing these questions, we find some remarkable results.

Specifically, in order to detect clustering on even finer scales and to determine more precisely the coherence times of drop size distributions, we look at 0.1-s and 0.01-s counts at different drop sizes. In the next section we first consider η and clustering for drops of one size. We then look at drops of different sizes, beginning with calculations of Ω and then searching for actual physical drop size distributions on the finest possible scales. Fi-

nally, for completeness we determine the geometric dimensionality of the flux of individual drop sizes and of the summation of all these fluxes, that is, the rain rate, using the box-counting technique.

2. Analysis of high-resolution video disdrometer data: Single drop sizes

To explore further, we consider the 18-min period of rain discussed in Parts IV and V (Jameson and Kostinski 1999a). While there was also a "transition" period of continuous but lighter rain, for clarity only the "main" events of rain are illustrated in Fig. 1. [As an aside, even the highly variable first rain event in Fig. 1a is accurately simulated using a statistically homogeneous (stationary) process in Part V, implying a wide tolerance in nature for the meaning of such terms. Correlated fluctuations should not be confused with nonstationary, "meteorological structure." See the appendix.]

Using the entire rain event, we first compute the pair correlation function η at 0.1-s resolution (Fig. 2) for drops having mean diameters of 0.625, 1.125, and 2.125 mm, the largest drop size with events occurring at a frequency sufficient for analyses. Obviously, there is clustering even over times of only 0.1 s. For the nominal terminal velocities corresponding to the largest and smallest diameters, this temporal scale then corresponds to vertical scales of 26–70 cm. (One might argue that these scales are too fine and that the appropriate distance scale should be that corresponding to the horizontal advection across the detector. However, even an advection speed of 10 m s^{-1} is of the same order as the terminal velocity of the largest drops so that such arguments are
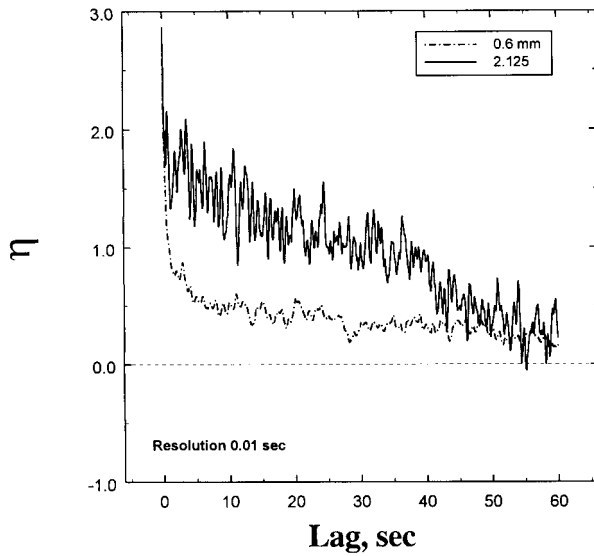
FIG. 3. The pair correlation function for the largest and smallest drop sizes for a temporal sampling of 0.01 s over the entire period of observations.
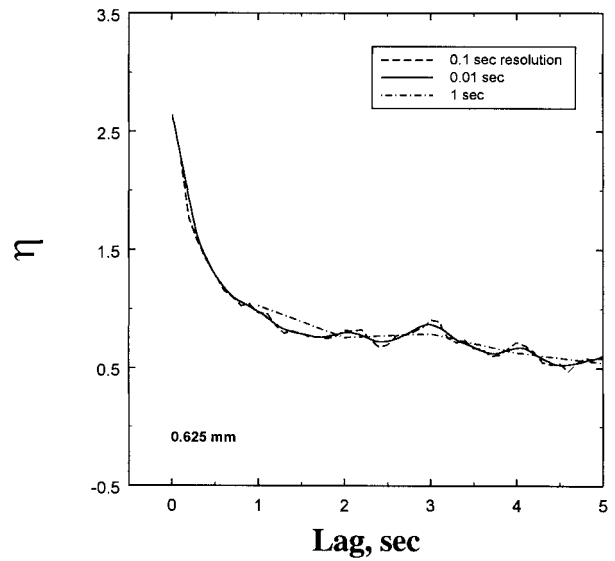

FIG. 4. An overlay of the pair correlation functions at three different temporal resolutions for 0.625-mm-diameter drops. There are no significant differences among them as η continues to increase at decreasing lags of ever finer resolutions.

really rather pedantic, particularly since clustering is occurring even over a few centimeters, as shown below.)

We next consider 0.01-s data and find that pair correlation is still occurring apparently even down to scales of 2.6–7 cm (Fig. 3). Note that the form of η is not significantly affected by changes in the resolution (Fig. 4) (see Kostinski and Jameson 2000, hereafter KJ00) with the important exception that clustering is still apparent at ever finer resolutions.

To demonstrate the meaning of η physically, we next consider a time segment in which the accumulation of counts of drops of one size appears to be quite steady, as illustrated in Fig. 5. The slope of this line corresponds to a mean flux of 2.314 s^{-1}. (Critical inspection shows that there are little wiggles, but that is precisely our point. Rain is never really smooth at resolutions below the coherence distance, that distance when η first crosses zero, for example.) Over this interval of "constant flux," the "counts" occurring during each 0.01 s are plotted in Fig. 6 and compared to those expected had each event (drop arrival) been statistically independent ("binomial" expectations). Obviously the observed counts in some intervals far exceed those expected assuming statistical independence. More precisely, the probabilities of seeing a count of three, four, or five drops in a single 0.01-s interval are 1.5×10^{-6}, 5.9×10^{-9}, and 1.3×10^{-11}, respectively. For the 21 000 0.01-s intervals in this example, then, one such event at the three, four, or five level should only occur at probabilities of 3 in 100, one in a million, and one in ten million, respectively. Consequently, the probabilities of the total number of events at the three, four, or five levels actually observed in Fig. 6a are only 3 in 100 billion, 7 in 10 trillion and one in 10 trillion, respec-

tively. Obviously, we must conclude that the *correlation and clustering of raindrops on these scales of a several centimeters is statistically very significant and real.* [It turns out that this is to be expected according to the fluctuation–correlation theorem (for discussion, see KJ00), which implies that clustering must occur on all scales less than the coherence length of η.] Hence, in answer to one of the two original questions, it appears that clustering indeed occurs on scales from several cen-
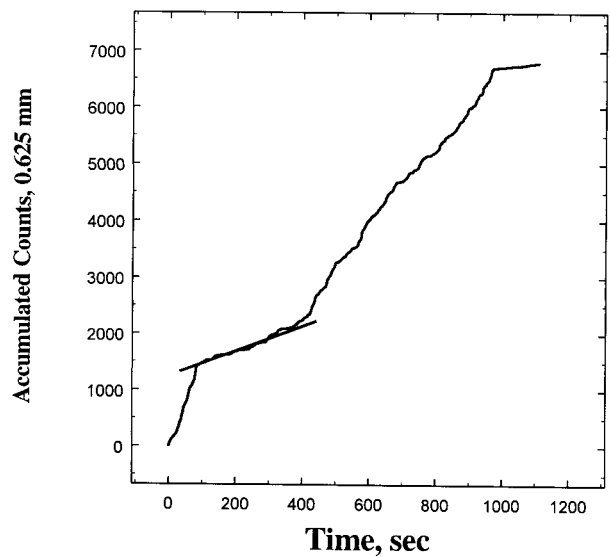

FIG. 5. The accumulated counts at 0.01-s resolutions for the entire period of observations. The line is through a region where the accumulated counts are increasing at a constant mean rate.
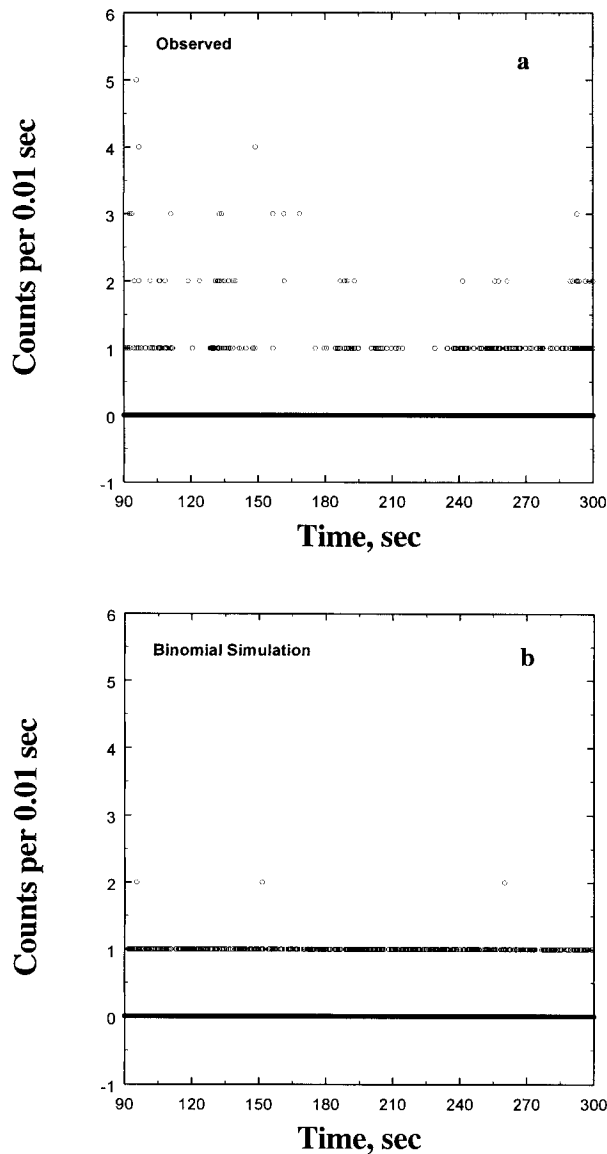
FIG. 6. (a) Counts per 0.01-s interval through the region of steady flux in Fig. 5 and (b) expected counts if the drops appeared completely independently of each other (uncorrelated) for the same mean flux of about one drop every 50 intervals. The differences are statistically highly significant (see text) so that clustering is occurring on time-scales corresponding to centimeters.

timeters (this work), to meters (this work and Part IV), up to a few kilometers (Part I).

But what about drops having different diameters? In the next section, we explore correlated behavior among different sizes of drops. In particular, we demonstrate the existence of physical drop size distributions apparently lasting, at times, no more than a few seconds. Even more significantly, it appears that the model of drop size distribution patches presented in Parts II and IV is valid. Some implications are also discussed below.
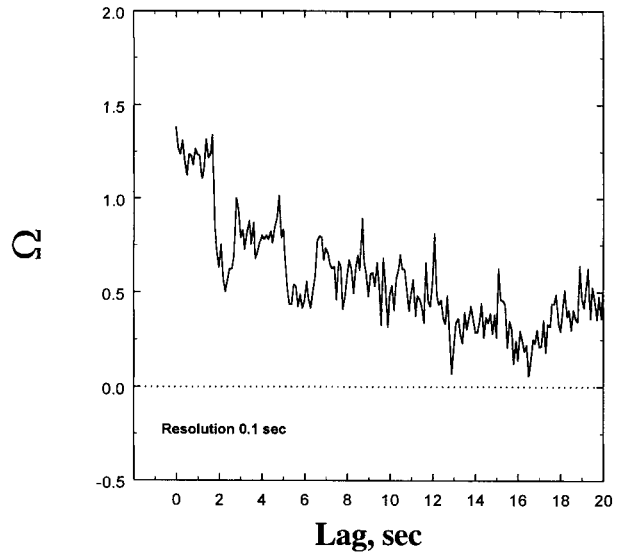

FIG. 7. The pair cross-correlation function between 0.625- and 2.125-mm-diameter drops at a temporal resolution of 0.1 s, indicating significant cross correlation even at scales as small as a few 0.1 s.

3. Analysis of high-resolution video disdrometer data: Multiple drop sizes

To begin, using the entire dataset, the pair cross-correlation function (Ω) between the largest and smallest sizes is illustrated in Fig. 7. Even at a temporal sampling of 0.1 s, significant cross correlation exists between these drops. Moreover, strong cross correlation still appears (Fig. 8) even when the resolution is reduced to only 0.01 s. These high-resolution observations suggest that it should be possible to identify coherent patches of physical drop size distributions over periods as brief
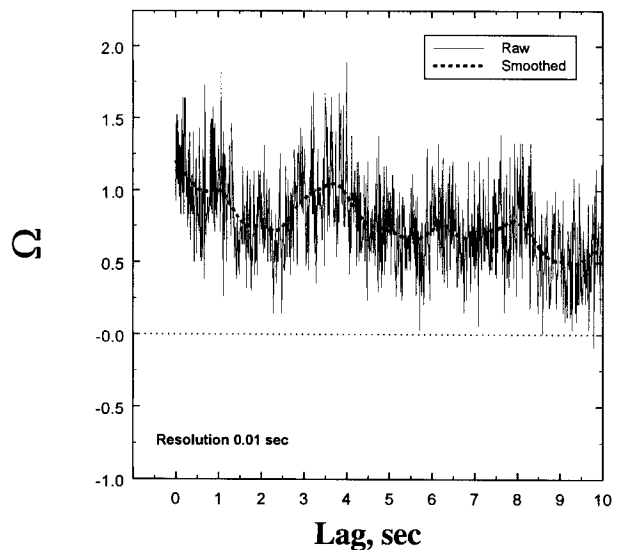

FIG. 8. Similar to Fig. 7 except that the resolution is 0.01 s, indicating that significant cross correlation exists even down to a few 0.01 s corresponding to distances of centimeters.
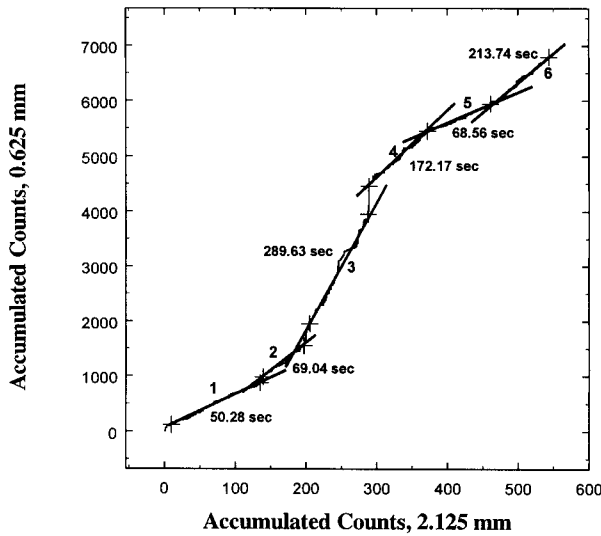
FIG. 9. Accumulated counts of 0.625-mm-diameter drops are plotted as a function of accumulated counts of those at 2.125-mm diameter. There are several regions of linear relations between the two counts consistent with the presence of steady drop size distributions. The times denote the duration of each linear region.
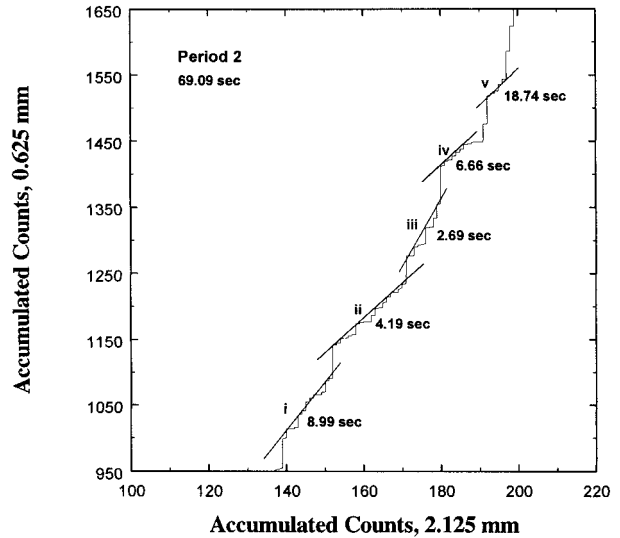

FIG. 10. An expanded plot of the linear region 2 in Fig. 9. Note the several smaller linear regions, some lasting only a few seconds. Also note the slopes of the lines change, indicating that the "slopes" of the distributions themselves are different.

as seconds. [While drop size distributions are normally computed for drop concentrations, we avoid uncertainties in the conversion from flux to concentration here simply by computing flux distributions directly. Such a procedure is justified in Part III of this series (Kostinski and Jameson 1999), where it is shown that the forms of the "flux" and "concentration" distributions are nearly identical over this range of sizes.]

The ratio of fluxes at two different sizes should remain constant for a well-defined drop size distribution so that accumulated counts at one size plotted as a function of those at another size should increase linearly. Such linearity, then, can be used to locate "stable" drop size distributions. For these data, the accumulated counts at the smallest and largest sizes are plotted in Fig. 9.

Within this rain there are indeed linear regions consistent with physical drops size distributions. However, within each of these regions, there appear to be even finer structures. As an illustration the particularly "smooth" location numbered 2 is enlarged in Fig. 10. Amazingly, there are even more readily identifiable, distinct small patches lasting on average only about 8 s (excluding transition spectra) but varying in duration from a mere 2.69 s up to 18.74 s. While Part IV hinted at likely subminute variations in the drop size distributions over tens of seconds, the brevity of some of these intervals is surprising. It is noteworthy that the slopes change from location to location and that these "regular" distributions are separated by transition spectra lacking numerous larger drops but showing an abundance of drops at the smaller sizes. While this finding

is encouraging, do these patches really represent coherent, physical drop size distributions?

Apparently they do. For example, the drop size distributions from period 2 for three such patches (increasing in durations by factors of 2 approximately) are illustrated in Fig. 11. Not only are the spectra well defined at 8.99 s, at 4.19 s, and even down to durations of only 2.69 s, they are also nearly exponential. Moreover, inspection shows that the transition distributions, which, in this example, last from a few to tens of seconds, consist of a greatly reduced total number of drops (n) associated with distributions having significantly steeper slopes (smaller average diameters $\overline{D}$). It is also worth noting that the regular distributions occur during more intense rainfall rates (in this case ~25–30 mm h⁻¹) as opposed to the transition spectra found when the rain rate is lighter (in this case ~2–5 mm h⁻¹).

There are at least two interesting implications. First, exponential distributions are thought to emerge as the result of drop coalescence and breakup only over considerable intervals (and distances) as the distribution approaches equilibrium. These times and distances, however, appear to be so long, in fact, that such equilibrium, exponential distributions are not even thought to exist in the real atmosphere (Srivastava 1971; Valdez and Young 1985; Hu and Srivastava 1995). We hypothesize here, however, that large-scale convection characterized by significant vorticity likely acts to concentrate or cluster drops into preferred regions so that drop size distributions perhaps may evolve toward exponential forms much more quickly that previously thought. On the other hand, they may simply be stochastic "accidents" brought about by some clustering mechanism.
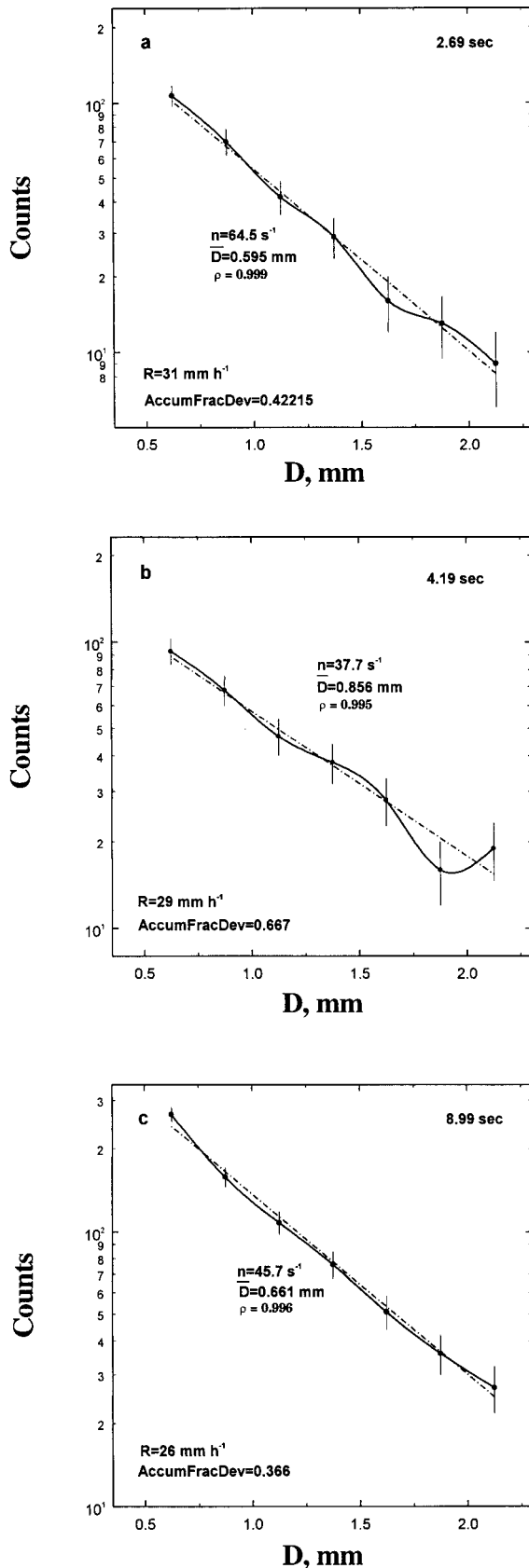
Second, if, as it appears, rain indeed consists of these short duration, physical drop size distributions having an exponential form lasting seconds, then the many reports of broader spectra such as gamma distributions can now be readily understood.

That is, such "observed" spectra are likely the result of a statistical mixing of other briefer, component distributions. These sometimes appear to be exponential of the form (Kostinski and Jameson 1999)

$$N(D) = n\left[\frac{1}{\overline{D}}\exp\left(-\frac{D}{\overline{D}}\right)\right], \tag{4}$$

where n is the total number of drops per unit volume and $\overline{D}$ is the mean drop diameter. [Note that the bracketed expression represents the probability density function (pdf) of D]. More precisely, most observed distributions are then likely of the form

$$N(D) = \int_0^\infty N(D|\overline{D})f(\overline{D})\,d\overline{D}$$

$$= \int_0^\infty \frac{n(\overline{D})}{\overline{D}}\exp\left(-\frac{D}{\overline{D}}\right)f(\overline{D})\,d\overline{D}, \tag{5}$$

where $f(\overline{D})$ is the probability distribution of $\overline{D}$ and $n(\overline{D})$ simply denotes the n that is associated with a particular $\overline{D}$ (i.e., contributing distribution). This can be expressed more clearly by letting $g(\overline{D}) = n(\overline{D})f(\overline{D})$ so that

$$\int_0^\infty g(\overline{D})\,d\overline{D} = \int_0^\infty n(\overline{D})f(\overline{D})\,d\overline{D} = \overline{N}.$$

Normalizing $g(\overline{D})$ by $\overline{N}$ so that $G(\overline{D}) = g(\overline{D})/\overline{N}$ integrates to unity from zero to infinity allows (5) to be written as

$$N(D) = \overline{N}\int_0^\infty \frac{1}{\overline{D}}\exp\left(-\frac{D}{\overline{D}}\right)G(\overline{D})\,d\overline{D}. \tag{6}$$

Although mixtures of other distributions are possible via (5), using (6) we can consider an observed drop size distribution that is a probability mixture of several exponential pdf's. One consequence of such mixing is that the variance is enhanced beyond that for a simple exponential. Specifically (Ochi 1990, 65–66),

$$\mathrm{var}[N(D)] = E_{\overline{D}}[\mathrm{var}(D|\overline{D})] + \mathrm{var}_D(E[D|\overline{D}]), \tag{7}$$

←

FIG. 11. Three drop size distributions corresponding to linear regions in Fig. 10 are plotted (solid lines). Poissonian error bars denote the one-standard-deviation uncertainty associated with each flux. Intervals were chosen to represent approximate powers (factors) of 2. Also included are the measured mean rainfall rate and the exponential distribution parameters (see text), as well as the correlation coefficient ρ. The accumulated fractional deviation from exponential (see Jameson et al. 1999; Kostinski and Jameson 1999, for details) are also given. The distributions appear to be highly exponential even over periods as small at 2–3 s corresponding to scales of around 20 m.

where the first term on the rhs of (7) may be associated with the "usual" variance for an exponential pdf of D [bracketed expression in the rhs of (4)], while the last term represents the enhancement due to the variance of $\overline{D}$ (and n associated with each $\overline{D}$).

As an illustration of such mixing, suppose $G(\overline{D})$ is a simple exponential of the form

$$G(\overline{D}) = \frac{1}{\mu} \exp\left(-\frac{\overline{D}}{\mu}\right), \qquad (8)$$

where μ is the average $\overline{D}$ during the entire interval for some $\overline{N}$. Substituting into (6) and integrating yields

$$N(D) = 2\overline{N}\sqrt{\frac{D}{\mu}}Y_1\left(2\sqrt{\frac{D}{\mu}}\right), \qquad (9)$$

where Y_1 is the modified Bessel function of the second kind (sometimes referred to as the Weber function). To illustrate, we set $\mu = 0.2$ mm and $\overline{N} = 234$ s^{-1} and plot the results in Fig. 12a. The curvature is reminiscent of some observed gamma distributions (Ulbrich 1983). In particular, for comparison we show actual disdrometer observations collected at Wallop's Island, Virginia, using a Joss–Waldvogel mechanical disdrometer during the passage of a squall as discussed in Kostinski and Jameson (1997) and Jameson and Kostinski (1998) (Fig. 12b). The similarity is striking. With different $G(\overline{D})$, mixing [i.e., (6)] likely yields a wide variety of distributions with different curvatures having different magnitudes.

It seems, therefore, that the spectrum of *measured* drop size distributions can be segmented into three regimes. At the finest measurement intervals, observations capture the apparently often exponentially shaped, physical distributions having durations from a few to several seconds. As the measurement intervals increase, however, there appears to be a gradual transition to more curved gammalike distributions (Ulbrich 1983), likely resulting from the mixture of several physical distributions as expressed by (5) and (6), for example. Finally, when averaging extends over very long intervals, the drop size distributions once again *return* to an exponential form because of statistical effects alone (Kostinski and Jameson 1999).

While it is not possible to illustrate the full range of spectra using these data, the transition from exponential, physical distributions to "mixture" distributions is apparent as illustrated in Fig. 13. As the measurement interval increases from about 3 to 1100 s, the exponential fit no longer falls within the one-standard-deviation error bars of the observations, and Fig. 13d shows a statistically significant curvature away from any pure exponential form.

These data also show a few other noteworthy features. In terms of the exponential parameters in (4) [viz., the total particle concentration (or flux) n and the average drop size $\overline{D}$] it is not $\overline{D}$ but rather n that changes most over time (Fig. 14). In these data, for example, it is the
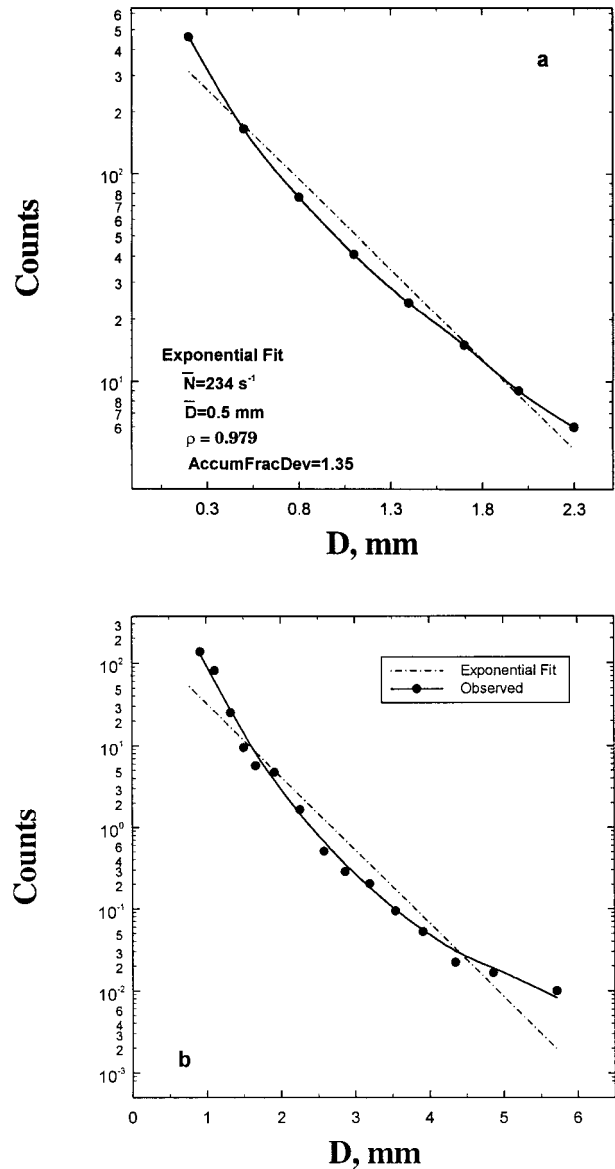

FIG. 12. (a) Plot of the drop size distribution (solid) resulting from a probability mixture of exponential distributions (see text) as compared to a fitted pure exponential (dot–dash). Note the curvature as a consequence of mixing distributions. (b) The observed distribution during the passage of a squall line at Wallops Island, VA (see Kostinski and Jameson 1997; Jameson and Kostinski 1998). Note the similar form of the two curves.

change in n that "explains" the factor of 5 difference in the measured rainfall rates between the shortest and longest measurement intervals. This is also illustrated as well in Fig. 15, showing n and $\overline{D}$ as functions of time over the entire period of observations. Whereas $\overline{D}$ is almost entirely confined to values from 0.5 to 1 mm, n varies by orders of magnitudes. In these data, then, it is n that is largely responsible for the variability in the rainfall rate (Fig. 1). That is, over short intervals, the rain really does arrive in true "bursts" or "gushes." It
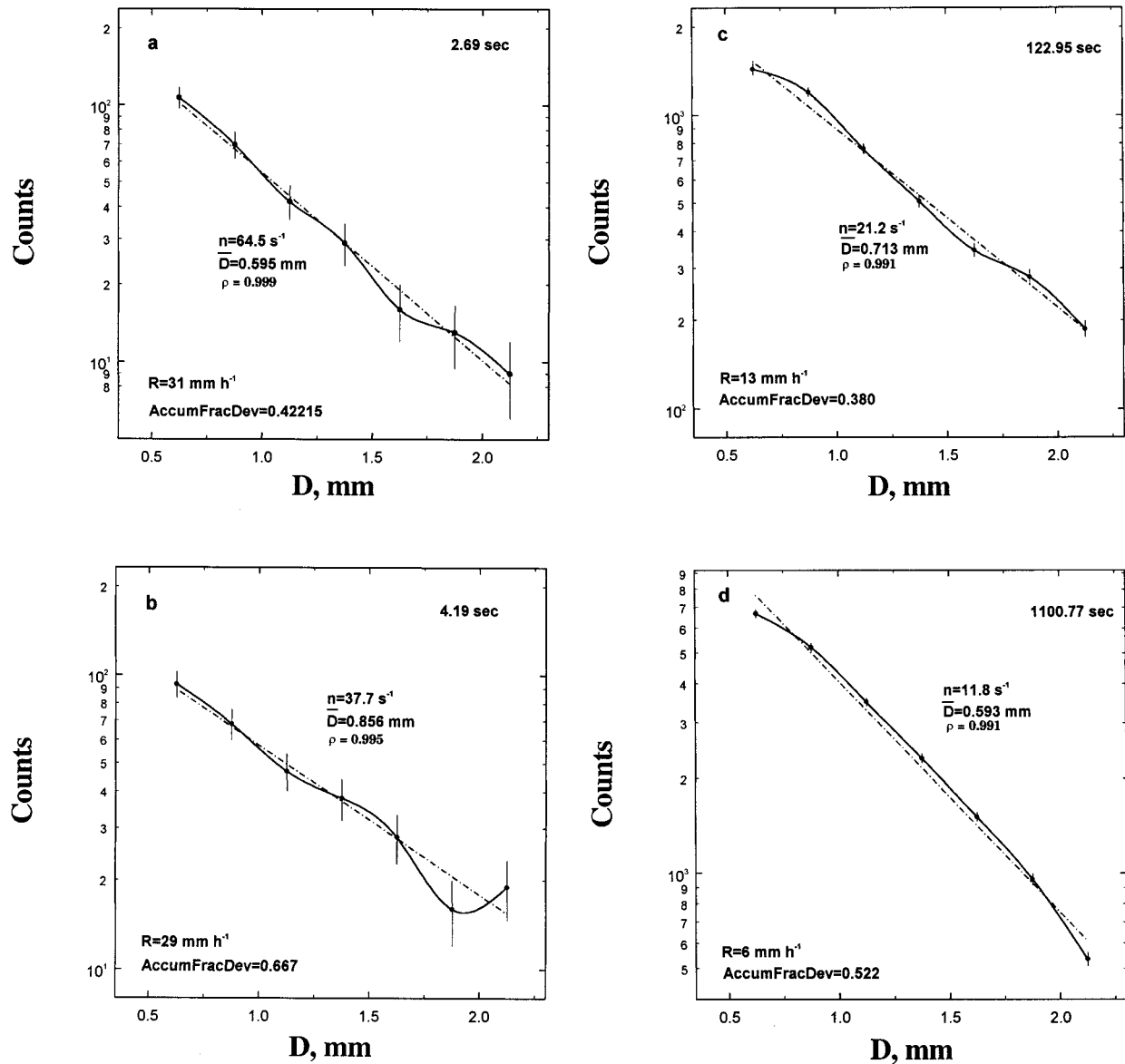
FIG. 13. A sequence of drop size distributions for increasing measurement intervals for (a) 2.69, (b) 4.19, (c) 122.95, and (d) 1100.77 s. The error bars are one standard deviation using Poissonian estimates in (a), (b), but using observations in (c), (d). Note the decreasing statistical significance of the exponential with increasing measurement interval. (c), (d) The effects of increased mixing of several physical distributions. Also note the change in the mean rainfall rates and in the total number flux for the exponential fit, n, even while $\overline{D}$ remains nearly constant (see Kostinski and Jameson 1999, 112).

is likely that many of the "spikes" in Fig. 1 are real and not simply statistical artifacts.[2]

It appears, then, that rain physically consists of relatively short-term drop size distributions that are often well matched by an exponential function. In the past, such physical distributions have not been observed be-

---

[2] The fluctuations in n are also likely responsible for much of the variability in the coefficients in Z–R relations, where Z is the radar reflectivity factor and R is the rainfall rate. Specifically, for a typical relation of the form $Z = aR^{1.35}$, it can be shown readily that $a \propto n^{-0.35}(\overline{D})^{0.88}$. While n may easily vary by factors of 10–100, $\overline{D}$ will vary at most by only around a factor of 2. In these data $\overline{D}$ remains nearly constant while n varies by a factor of 5 so that a changes by a factor of 1.75 in going from scales of meters to kilometers all

because of n. Moreover, since the expected values R and Z based on (19) in Kostinski and Jameson (1999) can be written as $E(R) \propto E(n)E(D^3 V_t)$, where V_t is the terminal fall speed while $E(Z) \propto E(n)E(D^6)$, the ratio $E(Z)/E(R)$ is independent of $E(n)$. That is, proper Z–R relations are linear and completely independent of drop concentration.
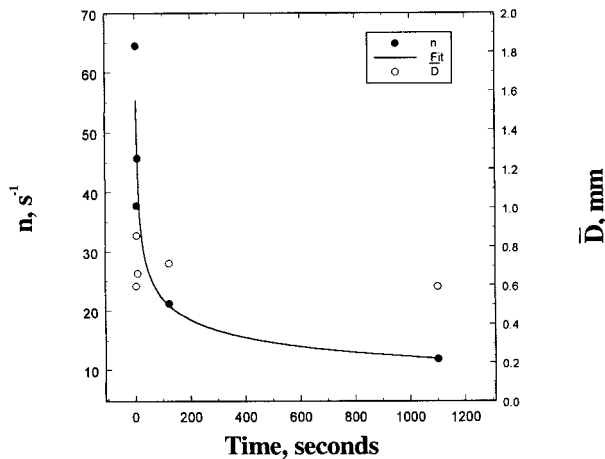
FIG. 14. The exponential parameters corresponding to Fig. 13 plotted as a function of time. Note weak changes in $\overline{D}$ over time compared to the large changes n.

FIG. 15. Time series of n and $\overline{D}$ for the entire period of observation. Whereas $\overline{D}$ lies within $\pm 33\%$ of the mean (0.75 mm), n varies over more than two orders of magnitude (100). Therefore, $\overline{D}^3$ (diameter contribution to the rainwater content) varies by about a factor of 2 $\ll$ 100. The cross-correlation coefficient between n and $\overline{D}$ is only -0.07, which is *not* consistent with $N_0 = n/\overline{D} =$ constant (implying n and $\overline{D}$ fluctuate in unison and, hence, exhibit strong positive correlation). It is, however, in agreement with simulations of the Waldvogel jumps reported in Kostinski and Jameson (1999).

cause the measurement interval normally extends from minutes to hours, days, and even seasons. Much of the discussion, then, has focused on the form of such "average" distributions. We suggest here that the brief, physical exponential-like distributions arise perhaps because of enhanced interactions in preferred regions of clustering. After all, convective turbulence is not just any random process, but rather is one characterized by enhanced vorticity. On longer measurement scales, other forms, such as the gamma distribution, arise because of a statistical mixing of many short duration, physical distributions over the measurement interval. As the averaging extends to even longer intervals, however, the distribution may once again appear exponential because of the emergence of complete statistical independence after averaging over a wide variety of conditions (Kostinski and Jameson 1999).

Aside from drop spectra, it appears that not only are raindrops of a single size clustered, but also that clustering among raindrops of different size is correlated leading to the clustering of rain and to rain gushes on scales from centimeters to kilometers. While such clustering is symptomatic of fractal structures, it is not a condition sufficient to justify such a purely geometric description of rain. Therefore, while of less significance but for the sake of completeness, in the next section we consider, briefly, the geometric dimensionality of these rain observations.

4. On the geometric dimensionality of rain

Obviously there is extreme variability associated with the patchiness of rain, as one should expect based on earlier work (Parts I–V). Yet in spite of this, it is possible to measure a geometric dimensionality using the usual "box-counting" methodology. To illustrate, we begin first with drops of one size. That is, starting with the first drop, we count the number of drops over a fixed
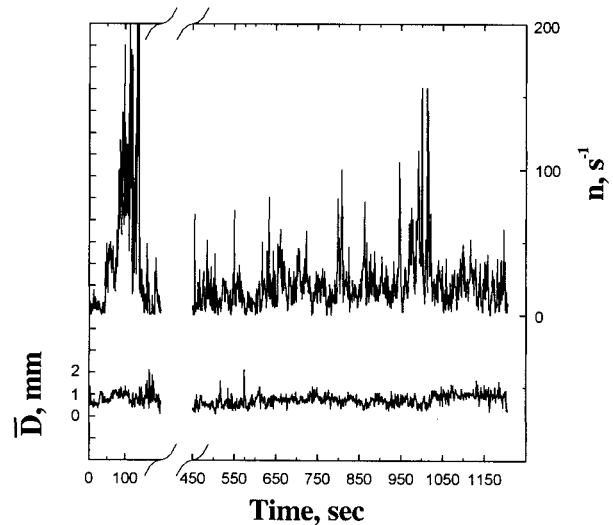
time interval. We then shift this "box" over one sampling resolution interval and count again. We then do this for all the data and compute the ensemble "average number" of drops corresponding to that resolution. Next, we increase (say, double, for illustration) the counting-box resolution. We would then expect that "normally," the ensemble average number of drops would double as well. However, if the rain were "fractal," the average number of drops in the sampling interval would increase only by a factor of, say, 1.6, instead of 2. Consequently, if the mean number of drops is plotted as a function of counting-box measurement length, then normal geometry would yield a line with the slope of unity. On the other hand, if the plot is curved and the logarithm of the number of counts versus the logarithm of the length of the resolution counting-box yields a line with a slope that differs from unity, then the geometry is fractal (e.g., see Lovejoy and Schertzer 1990). If, in this example, such a trend were to persist over all measurement resolutions, then the geometry of the rain structure would have a fractal dimension of 0.8 instead of unity.

In Fig. 16 the results of such a box-counting procedure using the video disdrometer data are shown for the two rain events illustrated in Fig. 1 for drops having a mean diameter of 0.625 mm. Excluding those regions at both ends of the timescale affected by sampling (at the smallest end by the limited number of drops and at the larger end by the limited number of samples (see Lovejoy and Schertzer 1990), we conclude that the flux-
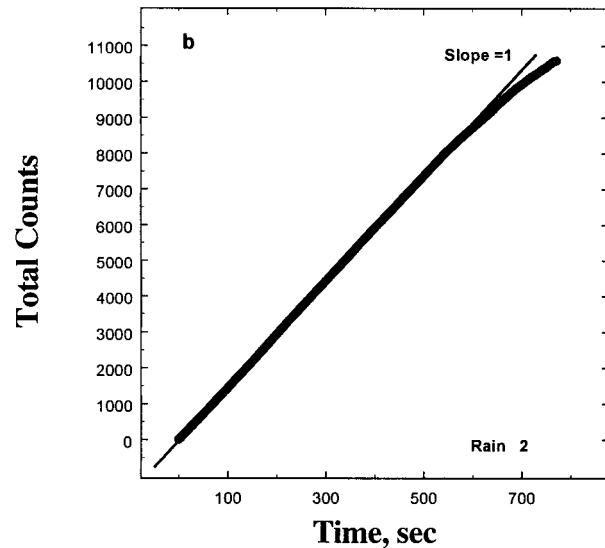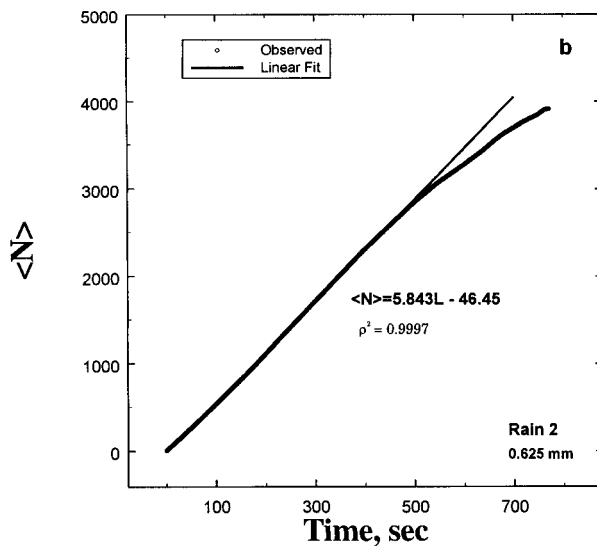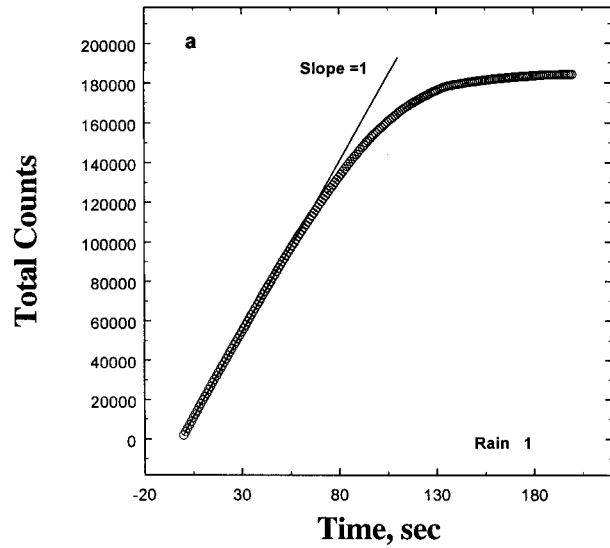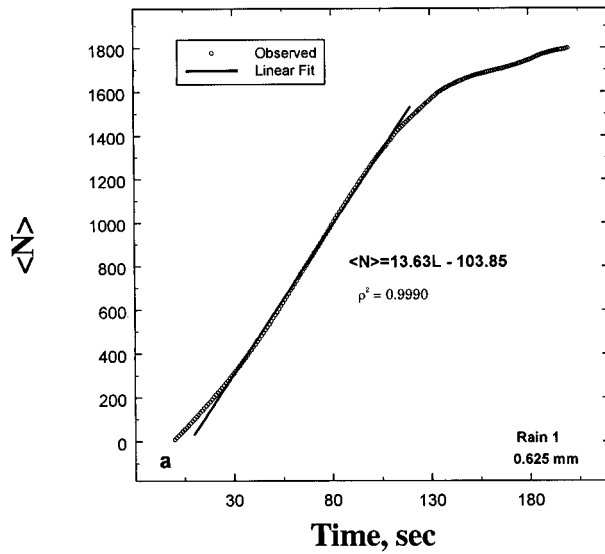
FIG. 16. The ensemble average number of 0.625-mm-diameter drops in the (a) first and (b) second rain events illustrated in Fig. 1 as a function of box-counting length in seconds. The durations of the two events were 201 and 773 s, respectively. Note the regions where counts are statistically reliable and the slope is unity.

FIG. 17. Similar to Fig. 15 except that the total counts (rain flux) are plotted. Again, where the counts are reliable, the slope is unity, indicating that the rain flux itself scales in an Euclidean manner.

es increase linearly [slope (power) of unity] so that these data are *not* fractal.

But rather than just restricting ourselves to drops of one size, consider instead the summation of fluxes over all sizes. This amounts to considering the dimensionality of the rainfall rate itself. These results are plotted in Fig. 17.

The total rain flux (rain rate) also appears to obey Euclidean (nonfractal) scaling at least in these measurements. Since the smallest time interval corresponds to 0.01 s while the longest duration with adequate sampling (Fig. 16b) lasts for 580 s, it appears that Euclidean

geometric scaling extends over scales from centimeters to several kilometers even in clustered rain.

5. Concluding discussion

In this series of articles we have attempted to take an unbiased and fresh look at the spatial–temporal nature of rain. In the course of these studies, we have applied many techniques from different fields of physical sciences. In that sense, much of what we have done is "not new" except for its application to physical meteorology. Yet, in the process, it is hoped that we have at least offered a rich alternative to the classic, uniform, Pois-

sonian perspective usually assumed in cloud and precipitation physics. In the process, many interesting questions concerning the meaning of statistical "homogeneity," "stationarity," and "average" have cropped up. When are conditions really stationary/homogeneous and when are they not? An answer is not always as transparent as it may seem at first inspection. For example, in Fig. 1a many would claim that the process is absolutely statistically "nonstationary." Yet the physical and statistical properties are accurately reproduced in a numerical simulation in which statistical stationarity is assumed (Part V, Jameson and Kostinski 1999a). The reason is that many processes that perhaps appear nonstationary may, in fact, be just a few realizations (coherence lengths) of a process that is fundamentally stationary over a length much greater than the duration of the observations, that is, lengths that are tens or hundreds of coherence intervals. Specifically, if some portion of a time series extends over only a few "coherence lengths," for example, correlated fluctuations may give the appearance of a deceptively "reasonable trend" in the data when, in fact, none exists (see the appendix for further discussion). If, on the other hand, a time series extends over many, many coherence lengths and there is still a clear and obvious trend, then the process may well be nonstationary. Nevertheless, as the appendix demonstrates, clustering and apparent structures *cannot* always be attributed to statistical inhomogeneity/nonstationarity.

In other respects, confusion arises because of the dominance of the Poissonian simplicity. For example, even after a rigorous explanation and acceptance as to why Poissonian statistics do not apply to a particular set of observations, we are then often immediately asked to demonstrate the statistical reliability of a measurement *in terms of Poissonian statistics.* The point we are trying to make, of course, is that the normal application of Poissonian statistics, such as the decrease of the relative variance with increasing drop concentration, usually does not apply to most observations of cloud droplets and raindrops. To reemphasize this, we briefly summarize the major points in this series of papers in hopes of providing a cohesive, overall perspective relevant to the structure of rain and clouds up to this moment.

In Part I (Kostinski and Jameson 1997), it is shown that drops of one size arrive in patches that exhibit enhanced concentrations (clustering) as a result of a doubly stochastic process in which not only the number of drops fluctuates, but so do the means. This perspective has met with objections that the "instantaneous" counts of the number of drops may well show non-Poissonian fluctuations, but still the "means" can be known simply by analyzing a time series of observations.

However, in response, the fact that a mean can be fit in retrospect does not preclude what actually happens in nature. That is, given past information, neither the mean nor the instantaneous counts are deterministic from one moment to the next. That is, the flux mea-

surement at one moment does not permit a meaningful prediction either of the mean nor of the instantaneous flux in the next moment. In that sense curves of the average, while easy to generate, are statistically meaningless in that they only appear to, but, in fact, cannot, separate a drop count into one component due to changes in the mean value and the other being a "random" variation. This is the key difference between our perspective and that of a nonhomogeneous Poisson process (Ochi 1990, p. 437) in which the mean varies in a deterministic fashion, for example. (See the appendix for an example that *cannot* be described by a nonhomogeneous process.) While ex post facto fits can be used to estimate averages, such curves can never really entirely separate fluctuations in the mean from other random fluctuations. Such information is simply not available. As it occurs in nature, therefore, it is our position that drop counts at one size must be viewed as a "doubly stochastic" process.

In Part II (Jameson and Kostinski 1998), this perspective is applied to different sizes of drops. It is demonstrated that drops having different diameters are simultaneously clustered and correlated. This leads to the natural identification of entities called physical drop size distributions that, because of their correlation, may in part be the consequence of drop interactions. These are to be distinguished from the oft reported "measured" or average distributions that represent a combination of many different physical distributions into some kind of mean size spectrum. As with Part I, however, the measurement interval is restricted to one minute so that a clear resolution of physical drop distributions on finer scales could not be explored.

In Part III (Kostinski and Jameson 1999a), it is noted not only that the frequently reported exponential drop size distribution can be cleanly separated into a concentration term times the pdf of the diameter, but also that over extensive averaging periods, a mean exponential distribution is to be expected strictly because of statistical independence and "lack of memory" regardless of any drop microphysics. It is also observed that the rainfall rate exhibits greatly enhanced fluctuations in clustered versus Poissonian ("steady") rain. Hence, steady rain can be defined according to whether or not the statistics of the drop counts are essentially Poissonian. We also note here that there is a slight anticorrelation (-0.07) between the total number density (n) and the mean drop diameter ($\overline{D}$) (see Fig. 15). This is *not* consistent with the Marshall–Palmer assumption (i.e., $N_0 = n/\overline{D}$ is a constant, as discussed in Part III, which in turn implies strong positive correlation between n and $\overline{D}$) and confirms results of simulations of the Waldvogel jumps presented in Part III.

A frequently repeated objection to the results in Parts I and II is that the long time series of 1-min Joss–Waldvogel disdrometer measurements "must" include effects induced by statistical nonstationarity. Still the entire 900-min time period contains between only 30

and 45 coherence intervals, making it virtually impossible to determine whether a particular meteorological structure is really associated with nonstationarity or is simply a manifestation of "correlated fluctuations" during a very long stationary process (see the appendix). Yet by confining much of the analyses in those two papers to intervals of only a few coherence lengths, it is not unreasonable to expect that any nonstationary mean component, if present, is likely to be changing only very slowly at most. The data and the analyses, then, should be dominated by "local," albeit perhaps correlated, fluctuations. Indeed, this view appears well vindicated by the detection of raindrop clustering over intervals as brief as a minute as demonstrated by the pair correlation and cross-correlation functions.

Nevertheless, we felt pressed to reduce the interval even further to minimize any potential influence of nonstationarity. Hence, in Part IV (Jameson et al. 1999), data are analyzed at greatly increased resolution using video disdrometer observations at an effective clock rate that is on the order of megahertz. Beginning conservatively, resolutions on the order of 1 s show that pair correlations for drops of one size as well as pair cross correlations among different sizes exhibit clustering on scales of meters. Moreover, physical drop size distributions exist and last over times of tens of seconds. These observations confirm the findings reported in Parts I and II. Yet even at 1-s intervals, it is clear that interesting processes are likely occurring at even finer resolutions.

In Part V (Jameson and Kostinski 1999a), simulations based on earlier results are used to demonstrate practical implications with regard to the statistical characteristics of the rainfall rate. More relevant here, however, is that simulations assuming statistical stationarity (homogeneity) accurately reproduce the highly variable conditions in Fig. 1a. Most of the variability is due to variations in the total number of drops with fluctuations in average drop size playing a relative minor role. It is also shown that, because of clustering, one can expect an increased frequency of both low and high rainfall rates. (That is, the rainfall rates are also clustered as we observe in this paper.) These findings conflict with a lognormal pdf of rainfall rates, which has a low frequency at small rain rates and too great a frequency at very large rain rates. Lognormal distributions, therefore, are not consistent with observations of the statistical physics occurring in natural, clustered rain.

Finally, then, we arrive at Part VI. In this paper, much finer temporal resolutions are used to demonstrate clustering and correlation on scales from centimeters to kilometers. That is, while rain appears to obey Euclidean scaling, it can still exhibit correlation and clustering. Thus, we believe that the proper characterization and simulation of clouds and rain is best approached using correlation functions and probability theory rather than through geometric considerations alone.

Furthermore, we have shown that rain consists of patches of coherent physical drop size distributions having diverse coherence times (distances) as proposed and discussed in the previous papers in this series. It also appears that in many instances over periods of several seconds these drop size spectra are well approximated by the exponential distribution. The detailed physics behind this is not entirely understood since normally "equilibrium" exponential drop size distributions are thought to be the results of drop collisions and breakup over extended periods often exceeding natural constraints. It seems reasonable, however, to propose that convective and turbulent high-vorticity structures somehow produce preferred locations where drops cluster. This likely leads to enhanced interactions among drops over relatively short times and, consequently, to exponential-like (albeit probably nonequilibrium) drop distributions.

Furthermore, because drop size distributions are normally measured over periods from several minutes to hours to days, these observed distributions are likely the consequence of combining, as a statistical mixture [(5) and (6)], many different physical distributions yielding results often described by the gamma distribution in the literature. In the extreme case when data are combined over very extended periods such as months and seasons, it is further argued (Kostinski and Jameson 1999) that the exponential distributions once again reappear but this time as a consequence of statistical rather than physical processes.

In short, then, this series of articles presents a new paradigm of rain that likely has important implications to cloud and precipitation physics, as well as to practical applications of remote sensing and hydrology. To name a few, the clustering of drops and patchiness of rain affects the signal statistics of many remote sensing instruments (Jameson and Kostinski 1996; Jameson and Kostinski 1999b), the characterization of the distribution of rain rates (Jameson and Kostinski 1999a), and even our understanding of the icing process (Jameson and Kostinski 2000).

Furthermore, algorithms requiring the combination of data using instruments with vastly different resolutions are also likely affected by the patchiness of the rain. A classic example is that of constructing radar Z–R relations of the form $Z = aR^b$. As discussed in the footnote, in conditions of natural clustering, gauges with 8-in. orifices "see" a rain with an a that is entirely different from that a radar sees over billions of cubic meters. While appreciated previously in terms of Poissonian statistics, we can only now begin to really understand and account for the true magnitude of these random characteristics of rain.

The essence of this work, then, is that while clustering is inevitable in statistically inhomogeneous/nonstationary processes, it also occurs even in statistically homogeneous/stationary processes on all scales less than the coherence length of either the pair correlation or autocovariance function. (If there are several such zero-

crossings, then clustering appears over several scales as well.) It is important to remember, however, that under some circumstances the size of the resolution volume may exceed the coherence length so that no correlation appears. Yet correlation and clustering may still be occurring on smaller scales. In such cases it is always important to check to see if the variance exceeds the mean by 10%–20%. If so, then correlation and clustering are still occurring but simply are not observable without finer resolution, as pointed out in KJ00.

APPENDIX

An Example of Non-Poisson Statistics and Raindrop Clustering in Statistically Stationary Rain

A common response when presenting this material is that whenever similar values of a quantity such as drop counts are found in a sequence of observations, for example, then the resulting structure must necessarily be the consequence of an inhomogeneous (nonstationary) statistical process. From this perspective, such observations must then, at some level, have a deterministic origin to be discovered given sufficient resolve and data resolution. This is the essence of attempts to describe such observations as a nonhomogeneous Poisson process (see Ochi 1990, 427). The alternative suggestion that such structures may simply be the expression of correlated fluctuations of a much longer statistically homogeneous (stationary) process are rarely considered. Yet the simple observation of structure is insufficient to distinguish between a stationary as opposed to a nonstationary processes, and, in fact, can be quite misleading. Wunsch (1999, 245) recently stated this in the following manner.

> But purely random processes, particularly those that have even mildly "red" spectra, have a behavior that comes as a surprise to many, and there is a great risk of misinterpretation. That is, the purely random behavior of a rigorously stationary process often appears visually interesting, particularly over brief time intervals, and creates the temptation to interpret it as arising from specific and exciting deterministic causes.

The reason that a distinction between stationary and nonstationary is important here is that deviations from Poisson statistics occur in both cases. For a statistically nonstationary process, the distribution of drop counts broadens, and correlations appear among counts in
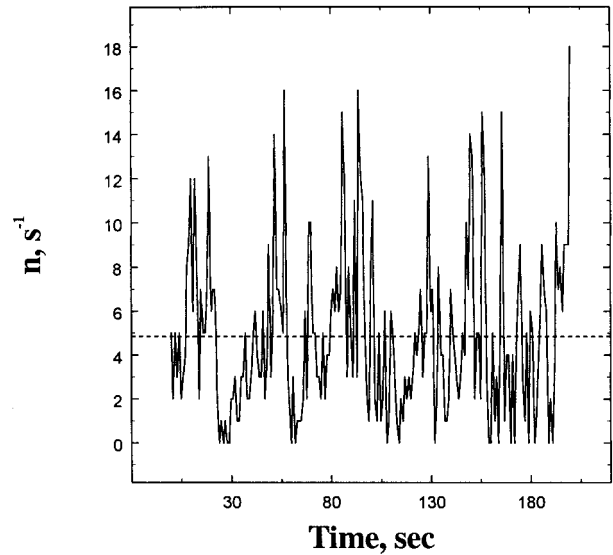

Fig. A1. The time series of 1-s counts of 0.625-mm-diameter drops observed using the video disdrometer for the period 460–660 s in Fig. 5. The dashed line denotes the mean value over the interval.

neighboring time intervals in a manner reminiscent of a mixture process (Kostinski and Jameson 1997) for a statistically stationary process. While this distinction seems somewhat academic with respect to the reality of raindrop clustering, such a question becomes paramount in the search for deeper understanding of the physical origins of clustering.
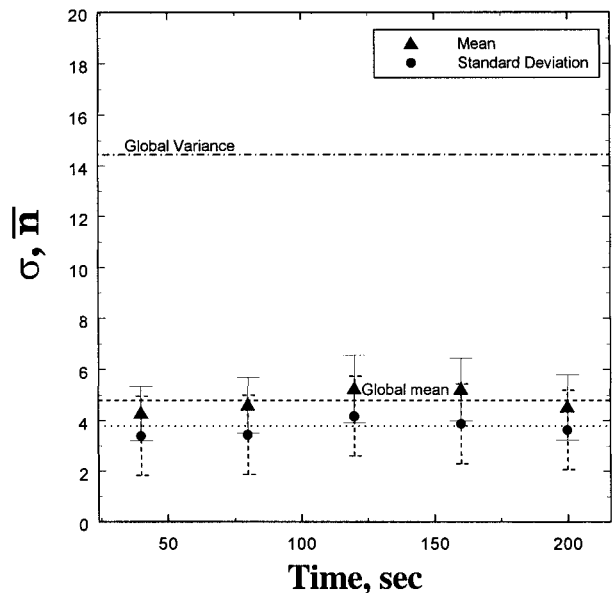

Fig. A2. The ensemble average of the mean ($\bar{n}$) number of counts per second and standard deviation (σ) for five 40-point groups of data. The constancy of σ and $\bar{n}$ indicate wide sense stationarity over the interval. Also note that the observed average variance (computed using each value individually) is over three times the mean, i.e., over three times that expected for a Poisson distribution.
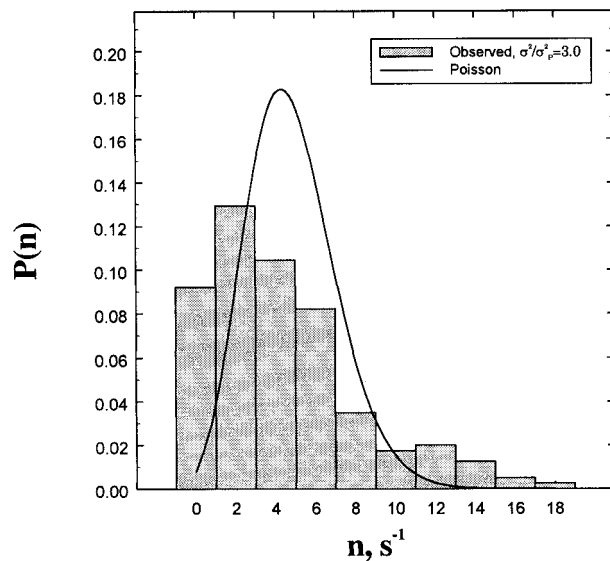
FIG. A3. The observed probability density distribution (bars) is compared to a Poisson distribution having the same mean as observed. Note the increased frequencies at both lower and higher counts compared to a Poisson distribution, indicating raindrop clustering and significant deviations from Poisson statistics. Also note that the observed variance σ^2 is three times larger than the Poisson variance (σ_P^2).

In that spirit, the purpose of this appendix is to provide an example of raindrop clustering and deviation from Poisson statistics during a wide sense stationary (the mean and variance are independent of origin) flux of 0.625-mm-diameter raindrops over a 201-s interval observed by the video disdrometer (460–660 s in Fig. 5). While a much longer period of observations will be sought in future data, we remind the reader that brevity alone cannot be invoked to dismiss these high-resolution measurements particularly by those who are then just as quick to embrace the ''clearly nonstationary'' nature of the 201-s event illustrated in Fig. 1a [an event, it turns out, just as readily recreated by correlated fluctuations of a statistically stationary process as demonstrated in Jameson and Kostinski (1999a)]. We also note that while this segment is only a fraction of the entire period, that does not mean that the sequence as a whole is nonstationary. It may well be that, like Fig. 1a where the variability is much greater, these data can still be considered the realization of a much longer stationary, random process exhibiting correlated fluctuations.

Figure A1 is the time series of drop counts illustrating the apparent constancy of both the mean and the variance, required for wide sense stationarity. This constancy is confirmed rigorously in Fig. A2. For the observed coherence length of 4 s, the mean and standard deviations are plotted as a function of five statistically independent groups each containing 40 data points having an ''effective'' number of 10 independent values. The error bars for the mean correspond to plus or minus one standard deviation computed using the variance

measured for each separate group assuming 10 independent values. The error bars for the standard deviation are calculated using the variance of the variance of the five sets of 40 points.

No statistically meaningful trends appear in these data; that is, the mean and standard deviation remain constant. It is noteworthy, however, that the global variance is still three times the mean; that is, it is three times the variance for a Poisson distribution. This suggests raindrop clustering and a non-Poisson distribution of drop counts.

Such a conclusion is substantiated by looking at the density distributions of counts illustrated in Fig. A3. The deviation of the observed distribution from the Poisson is obvious in both the enhanced frequencies at low counts and at higher counts. It is no accident, then, that the variance of the observed distribution is three times that of the ''equivalent'' Poisson distribution, that is, the Poisson distribution having the identical mean (with the variance equal the mean).

Hence, this example illustrates that raindrop clustering does occur in the atmosphere in statistically stationary conditions as proposed in Kostinski and Jameson (1997), Jameson and Kostinski (1998), KJ00, and Jameson et al. (1999). Moreover, these observations *cannot* be explained in terms of a nonhomogeneous Poisson process.

Regardless of the origin of the clustering, however, it should be remembered that these same works show the existence of raindrop clustering over a wide range of scales.

REFERENCES

Green, H. S., 1969: *The Molecular Theory of Fluids.* Dover, 737 pp.
Hu, A., and R. C. Srivastava, 1995: Evolution of raindrop size distribution by coalescence, breakup, and evaporation: Theory and observations. *J. Atmos. Sci.,* **52,** 1761–1783.
Jameson, A. R., and A. B. Kostinski, 1996: Non-Rayleigh signal statistics caused by relative motion during measurement. *J. Appl. Meteor.,* **35,** 1846–1859.
——, and ——, 1998: Fluctuation properties of precipitation. Part II: Reconsideration of the meaning and measurement of raindrop size distributions. *J. Atmos. Sci.,* **55,** 283–294.
——, and ——, 1999a: Fluctuation properties of precipitation. Part V: Distribution of rain rates—Theory and observations in clustered rain. *J. Atmos. Sci.,* **56,** 3920–3932.
——, and ——, 1999b: Non-Rayleigh signal statistics in clustered statistically homogeneous rain. *J. Atmos. Oceanic Technol.,* **16,** 575–583.
——, and ——, 2000: The effect of stochastic cloud structure on the icing process. *J. Atmos. Sci.,* in press.
——, ——, and A. Kruger, 1999: Fluctuation properties of precipitation. Part IV: Finescale clustering of drops in variable rain. *J. Atmos. Sci.,* **56,** 82–91.
Joss, J., and A. Waldvogel, 1967: Ein Spektrograph für Niederschlagstropfen mit automatischer Auswertung. *Pure Appl. Geophys.,* **68,** 240–246.
Kostinski, A. B., and A. R. Jameson, 1997: Fluctuation properties of precipitation. Part I: On deviations of single-size counts from the Poisson distribution. *J. Atmos. Sci.,* **54,** 2174–2186.
——, and ——, 1999: Fluctuation properties of precipitation. Part

III: On the ubiquity and emergence of the exponential drop size spectra. *J. Atmos. Sci.,* **56,** 111–121.

——, and ——, 2000: The spatial distribution of cloud particles. *J. Atmos. Sci.,* in press.

Lovejoy, S., and D. Schertzer, 1990: Fractals, raindrops, and resolution dependence of rain measurements. *J. Appl. Meteor.,* **29,** 1167–1170.

Ochi, M., 1990: *Applied Probability and Stochastic Processes.* John Wiley and Sons, 499 pp.

Sheppard, B. E., and P. I. Joe, 1994: Comparison of raindrop size distribution measurements by a Joss–Waldvogel disdrometer, a PMS 2DG spectrometer, and a POSS Doppler radar. *J. Atmos. Oceanic Technol.,* **11,** 874–887.

Srivastava, R. C., 1971: Size distributions of raindrops generated by their breakup and coalescence. *J. Atmos. Sci.,* **28,** 410–415.

Ulbrich, C. W., 1983: Natural variations in the analytic form of the raindrop size distribution. *J. Climate Appl. Meteor.,* **22,** 1764–1775.

Valdez, M. P., and K. C. Young, 1985: Number fluxes in equilibrium raindrop populations. *J. Atmos. Sci.,* **42,** 1024–1036.

Wunsch, C., 1999: The interpretation of short climate records, with comments on the North Atlantic and Southern Oscillations. *Bull. Amer. Meteor. Soc.,* **80,** 245–255.